AMSI
AUSTRALIAN MATHEMATICAL SCIENCES INSTITUTE

National Collaboration in the Mathematical Sciences

Modelling the Evaporation of a Liquid Droplet

Joel Alroe
Supervised by A/Prof T. Farrell and Dr S. Psaltis
Queensland University of Technology

February 2013

Abstract

This report explores the development of a one-dimensional mathematical model for the evaporation of a pure liquid droplet suspended in its own vapour. In an attempt to account for all relevant transport mechanisms, a "first principles" approach is taken by developing the model from fundamental conservation equations. With the aid of a perturbation analysis, a reduced system of equations is achieved and solved numerically with MATLAB. Realistic responses to varying environmental conditions are demonstrated in several simulations. Finally, an imbalance in the heat flow across the liquid/vapour interface is established as the primary mechanism driving the evaporation process.

1 Introduction

Droplet evaporation is of great importance to diverse applications such as: pesticide dispersal, fuel combustion, and the fabrication of nanomaterials. The evaporative process is well understood from a broad perspective; however, it is becoming increasingly important to develop detailed and specific models that can simulate how the droplet evolves over time. This is no trivial task as the evaporation process is affected by a great number of parameters and environmental conditions. Common simplifications include assuming that the process will be dominated by particular flows, such as in the case of purely diffusive models, or applying empirically determined relationships.

The primary aim of this project is to begin with the fundamental conservation principles and, with minimal assumptions, derive an effective model for droplet evaporation. This model will then be used to investigate the effect of varied environmental conditions and the underlying mechanisms driving the evaporation process.

2 Model

We begin by considering a pure liquid droplet, suspended in an atmosphere of its own pure vapour, within a sufficiently large vessel and free from any external forces such as gravity. The radial symmetry of this physical scenario leads to a two phase, one dimensional model as depicted in Figure 1.

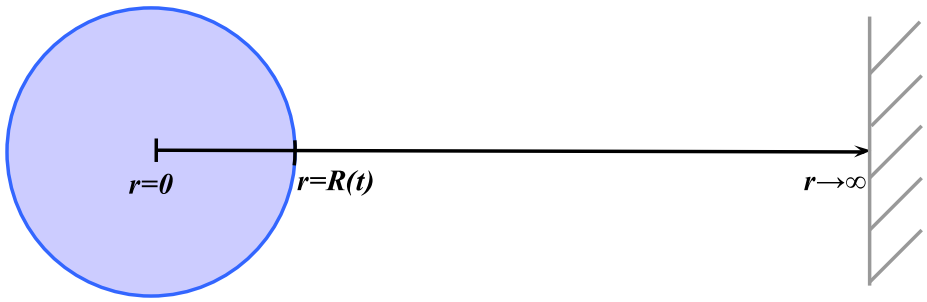

Figure 1: One dimensional domain for the droplet evaporation problem

Systems of equations are established in each phase, from the principles of conservation of mass, momentum and energy. According to the work of Bird, Stewart and Lightfoot [1], these conservation equations take the following form.

$$\text{Mass:} \qquad \frac{\partial \rho}{\partial t} = -\frac{1}{r^2}\frac{\partial}{\partial r}[r^2 \rho u] \tag{1}$$

$$\text{Momentum:} \qquad \frac{\partial \rho u}{\partial t} = -\nabla \cdot (\rho u^2) - \nabla p - [\nabla \cdot \boldsymbol{T}] \tag{2}$$

$$\text{Energy:} \qquad \rho \hat{c}_v \frac{DT}{Dt} t = -(\nabla \cdot q) - T \left(\frac{dp}{dT}\right)_{\hat{V}} (\nabla \cdot u) - (\boldsymbol{T} : \nabla u) \tag{3}$$

where ρ is the density, u is the velocity, p is the pressure, $\boldsymbol{T}$ is the stress tensor, $\hat{c}_v$ is the volumetric heat capacity, q is the heat flux, T is the temperature and $\hat{V}$ is the specific volume.

To establish outer boundary conditions, we prevent any flows at the centre of the droplet and apply Dirichlet boundary conditions at the far vapour boundary, as it is sufficiently distant to be unaffected by the droplet over time. In accord with derivations by Lock [4], boundary conditions are applied across the liquid/vapour interface which enforce continuity of temperature and mass, momentum and energy flux.

It is also necessary to include the Clausius-Clapeyron equation [4] to provide a relationship between temperature and pressure at the interface, during the phase change process. The general form of this equation assumes equal pressures across the interface. To avoid this assumption, we refer to Lock's [4] examination of the continuity of the specific Gibbs function. For each phase, we can express the total time derivative of this function as:

$$\frac{d\hat{G}}{dt} = \hat{V}\frac{dp}{dt} - \hat{S}\frac{dT}{dt} \tag{4}$$

where $\hat{G}$ is the specific Gibbs function, $\hat{V}$ is the specific volume, p is the pressure, $\hat{S}$ is the specific entropy and T is the temperature. Assuming continuity of the specific Gibbs function across the interface, we can equate the above equation on either side of the interface. Next, we apply the following substitutions:

$$L = T_v(\hat{S}_v - \hat{S}_l) \tag{5}$$

$$\hat{V} = \frac{1}{\rho} \tag{6}$$

where L is the latent heat of vaporisation, ρ is the density, and the l and v subscripts refer to the liquid and vapour phases. With some further manipulation, we arrive at the following modified form of the Clausius-Clapeyron equation:

$$\frac{1}{\rho_v}\frac{dp_v}{dt} - \frac{1}{\rho_l}\frac{dp_l}{dt} = \frac{L}{T_v}\frac{dT_v}{dt} \tag{7}$$

Collectively, these equations and boundary conditions form a closed system; however, solving such a highly coupled and non-linear system presents a formidable task and some simplifications are necessary.

Firstly, we assume that the vapour can be modelled as an ideal gas and that the liquid is an incompressible fluid. The former assumption removes vapour pressure from the list of parameters by relating it to density and temperature through the ideal gas law. The incompressible fluid assumption leads to three corollary assumptions: constant liquid pressure, no mass flow within the droplet and no viscous stresses in either phase. As a result, both the conservation of mass and momentum equations can be eliminated from the liquid phase.

Next, the remaining equations and boundary conditions are non-dimensionalised. This removes their dependence on units of measurement, groups any scaling constants as coefficients and allows an order of magnitude analysis to be performed. As a result, two coefficients are found to be very small, relatively speaking. The first of these, $\frac{1}{\nu_2}$ occurs in the following conservation of momentum equation for the vapour phase.

$$\frac{1}{\nu_2}\rho_v\left[\frac{\partial u_v}{\partial t}+u_v\frac{\partial u_v}{\partial r}\right]=-\frac{\partial(\rho_v T_v)}{\partial r} \tag{8}$$

This implies that any changes in vapour pressure are insignificant. The second small coefficient, ν_{11}, can be seen in the following interfacial boundary condition, derived from the continuity of momentum.

$$\rho_v T_v = p_l - \frac{\nu_{10}\sigma}{R}+\nu_{11}u_v\frac{dR}{dt} \tag{9}$$

This equation describes a balance of forces at the interface. Therefore, the negligible magnitude of ν_{11} implies minimal contribution from vapour evaporating from the surface of the droplet. To test the significance of these terms, a perturbation expansion is conducted, as outlined by Bush [2]. This reduces equation (8) to a simple statement of the isobaric condition in the vapour phase. With this result and some further manipulation of the equations, a significantly reduced system is achieved which relies only on the conservation of heat in the liquid phase, and conservation of mass in the vapour phase.

In order to numerically solve the system, it is convenient to fix the moving interface by applying a spatial scaling. The following Landau scaling was an approach used by Crank [3], where x becomes the scaled spatial parameter and $R(t)$ is the position of the moving interface.

$$r = xR(t) \tag{10}$$

This scaling is ideal within the droplet but not within the vapour phase. As the droplet radius diminishes, the Landau scaling progressively reduces the relative size of the vapour phase, and the Dirichlet boundary condition becomes increasingly inaccurate. Therefore it is necessary to apply the following spatial translation in the vapour phase to maintain a fixed interface position:

$$r = x + R(t) - 1 \tag{11}$$

In total, these simplifications and spatial transformations result in the following reduced system of equations:

Liquid phase (Conservation of heat)

$$\frac{\partial T_l}{\partial \tau} = \frac{\dot{R}x}{R}\frac{\partial T_l}{\partial x} + \left(\frac{\nu_1}{R^2x^2}\right)\frac{\partial}{\partial x}\left[x^2\frac{\partial T_l}{\partial x}\right] \tag{12}$$

Vapour phase (Conservation of mass)

$$\frac{\partial}{\partial \tau}\left[\frac{1}{T_v}\right] = \dot{R}\frac{\partial}{\partial x}\left[\frac{1}{T_v}\right] - \frac{\nu_3}{(1+\nu_4)r^2}\frac{\partial}{\partial x}\left[\frac{r^2}{T_v}\frac{\partial T_v}{\partial x}\right] \tag{13}$$

Initial conditions:

$$T_l(x,0) = 1 \qquad ; \qquad T_v(x,0) = 1 \qquad ; \qquad R(0) = 1 \tag{14}$$

Outer boundary conditions:

$$\frac{\partial T_l}{\partial x}(0,t) = 0 \qquad ; \qquad \lim_{x\to\infty} T_v(x,\tau) = 1 \tag{15}$$

Boundary conditions at the droplet surface:

$$T_l = \nu_5 T_v \qquad ; \qquad T_v = T_i \exp\left(\frac{\nu_{10}\sigma}{\nu_8\nu_9}\left(1 - \frac{1}{R}\right)\right) \tag{16}$$

$$\dot{R} = \frac{1}{\nu_7}\left(\nu_6\frac{\partial T_l}{\partial x} - \frac{\partial T_v}{\partial x}\right) \qquad ; \qquad T_i = \frac{L}{\hat{R}}\left(\frac{T_b}{\frac{L}{\hat{R}} - T_b\, ln(\frac{p_v}{p_b})}\right) \tag{17}$$

We now apply spatial and temporal discretisations to allow the system to be solved numerically. As discussed by Patankar [6], the conservative nature of these equations is well suited to a control volume scheme for spatial discretisation. For equation (12), this is implemented by integrating across the control volume, providing the following result:

$$\frac{\partial T_p}{\partial \tau} = \frac{3}{x_e^3 - x_w^3}\left[\frac{(x_e^4 - x_w^4)}{4}\frac{\dot{R}}{R}\frac{\partial T_p}{\partial x} + \frac{\nu_1}{R^2}\left(x_e^2\frac{\partial T_e}{\partial x} - x_w^2\frac{\partial T_w}{\partial x}\right)\right] \tag{18}$$

where e and w subscripts refer to values at the east and west face of the control volume, and the p subscript refers to values at the central node. To manage the non-linear terms, is has been necessary to assume that the temporal derivative of T_l on the left hand side and the spatial derivative in the advective term are approximately constant across the control volume.

Temporal discretisation is now applied by integrating equation (18) over a discrete timestep with an implicit Eulerian method, to minimise instability. In this case, we address the non-linearity in the advective term by lagging the spatial derivative and using its value from the previous iteration.

$$T_p^{n+1} - T_p^n = \frac{3}{x_e^3 - x_w^3}\left[\frac{x_e^4 - x_w^4}{4}\frac{\partial T_p^m}{\partial x}\ln\left(\frac{R^{n+1}}{R^n}\right) + \frac{\Delta\tau\,\nu_1}{(R^{n+1})^2}\left(x_e^2\frac{\partial T_e^{n+1}}{\partial x} - x_w^2\frac{\partial T_w^{n+1}}{\partial x}\right)\right] \tag{19}$$

A similar process is likewise applied to equation (13); however, an averaging scheme and lagging are required for the non-linearity within the diffusion term.

Finally, a numerical solver is written in MATLAB, which applies Newton's method to iteratively solve for droplet radius and temperature at each timestep. This solver utilises mesh refinement in the vicinity of the interface to improve the accuracy of finite volume approximations and achieves efficient, stable convergence of the solution at each timestep through adaptive timestepping.

3 Results

In order for this model to be valid, it must behave according to established rules of droplet evaporation. In particular, it needs to demonstrate appropriate responses to

environmental conditions and we expect it to follow the D^2 law, as discussed by McGaughey and Ward [5]. This law predicts that the square of the droplet diameter (or radius) will change linearly over time. To investigate this behaviour, an initial simulation was performed for a $100\mu m$ water droplet with 50% relative humidity and both phases initially at 50°C. As demonstrated in Figure 2 and Figure 3, the droplet evaporated completely within 20 seconds and the square of its radius closely approximated a linear trend, providing support for the model.

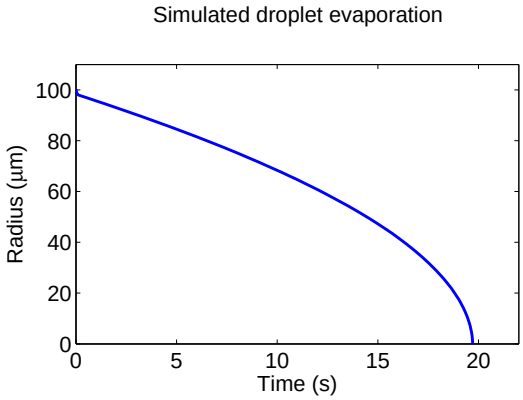

Figure 2: Radius of an evaporating droplet

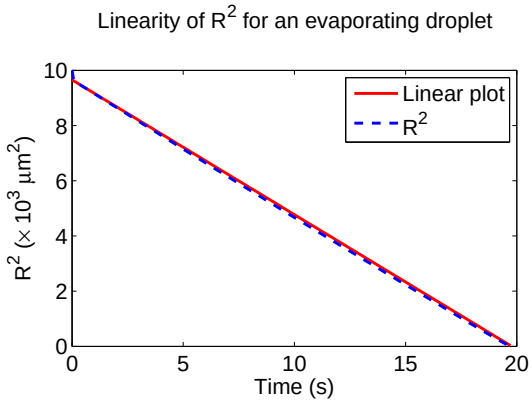

Figure 3: Comparison of the square of radius to an arbitrary linear function

In order to investigate the response to environmental conditions, two sets of simulations were performed for the same $100\mu m$ water droplet under varying relative humidity and initial temperature. For the simulations depicted in Figure 4, the droplet was subjected to relative humidities of 20%, 50% and 80%, with both phases initially at 50°C. Clearly, increasing humidity resulted in slower evaporation rates. This agrees with our understanding that evaporation slows as the vapour content in the surrounding atmosphere approaches the saturated vapour pressure.

As shown in Figure 5, the relative humidity was then maintained at 50% and the initial temperature across both phases was changed between 5°C, 30°C and 50°C. In this case, decreasing temperature slowed the rate of evaporation and at 5°C, the droplet instead experienced condensation. Each of the above simulations resulted in the expected linear change in the square of the radius and demonstrated appropriate changes to the evaporation rate for the environmental conditions. This sufficiently confirmed the validity of the model.

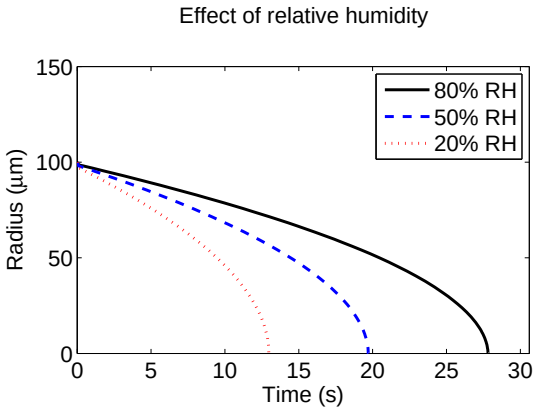

Figure 4: Droplet evaporation times increasing with relative humidity

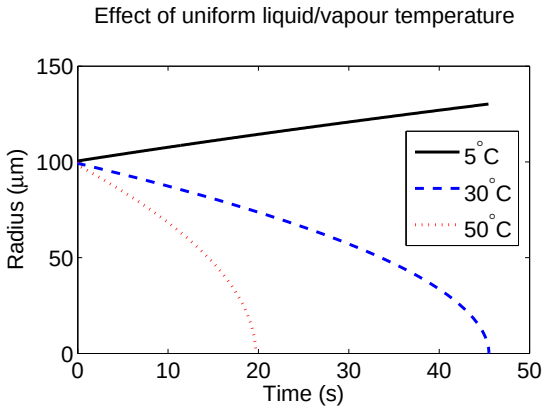

Figure 5: Droplet evolution over time for uniform initial temperatures

For comparison, a simulation was conducted with an initial vapour temperature of 30°C and a liquid temperature of 5°C. While this unsurprisingly resulted in complete evaporation, Figure 6 demonstrates a brief period of condensation observed during the first second of the simulation. We can investigate this unexpected result by examining the evolution of temperature profiles in the vicinity of the liquid/vapour interface. As shown in Figure 7, the temperature throughout the liquid phase required less than half a second to reach the same level as at the interface. At this point, the entire liquid phase was at a uniform temperature and thus no heat flow could occur from the interface into the liquid; however, the steep temperature gradients in the vapour phase guaranteed heat flow from the vapour into the interface. Therefore, in order to avoid violating conservation of energy, it was necessary for the interface to move left into the liquid phase. Clearly the imbalance in heat flux was the mechanism driving the evaporation process. Extending this thought process, the initial period of condensation likewise indicates that greater heat flow was entering the liquid phase than was being supplied by the vapour phase, necessitating a corresponding increase in droplet radius.

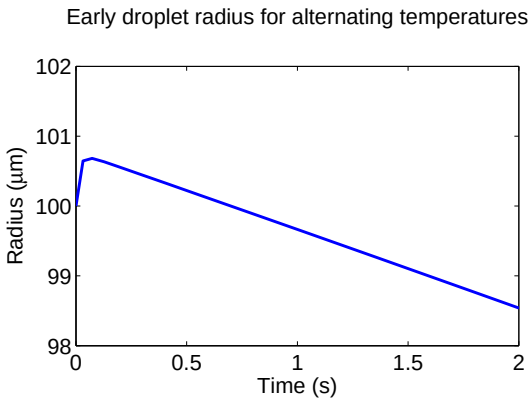

Figure 6: Early droplet evolution with initial vapour temperature higher than liquid temperature

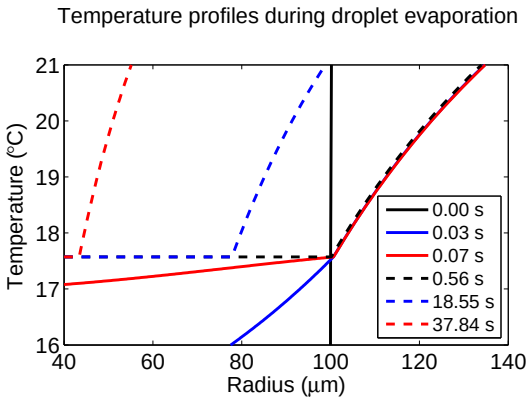

Figure 7: Temperature profiles near the liquid-vapour interface

4 Conclusion

The fundamental conservation principles for mass, momentum and energy were sufficient to develop a model for the evaporation of a pure droplet within its own vapour. Although a limited set of assumptions were required to assist with the numerical analysis, the model demonstrated realistic response to temperature and humidity and consistent agreement with the D^2 law. Furthermore, the model actively demonstrated that evaporation and condensation are ultimately governed by imbalances in heat flow across the liquid/vapour interface and the necessity for conservation of heat to be maintained.

This relatively simplistic scenario offers many options for further research. In particular, for spray pyrolysis applications, it would be important to examine the effect of vapour flows on convective transport and droplet deformation. Within the droplet, the effect of internal currents and chemical interactions between dissolved species would have great significance within the field of nanofabrication.

5 Acknowledgements

I enjoyed the project and had a great experience with the Big Day In. The Vacation Research Scholarship has helped broaden my mathematical knowledge and opened my eyes to the wide variety of mathematical research topics that are currently undertaken.

I would like to thank my supervisors A/Prof Troy Farrell and Dr Steven Psaltis for their endless support and enthusiasm during this project. I would also like to thank AMSI and CSIRO for their generous funding and for hosting the Big Day In.

6 Bibliography

References

[1] R. B. Bird, W. E. Stewart, and E. N. Lightfoot. *Transport phenomena.* John Wiley & Sons, New York, NY, 2nd edition, 2007.

[2] A. W. Bush. *Perturbation methods for engineers and scientists.* CRC Press, Boca Raton, FL, 1992.

[3] J. Crank. *The mathematics of diffusion.* Oxford University Press, New York, NY, 2nd edition, 1975.

[4] G. S. H. Lock. *Latent heat transfer: an introduction to fundamentals.* Oxford University Press, New York, NY, 2nd edition, 1994.

[5] A. J. H. McGaughey and C. A. Ward. Temperature discontinuity at the surface of an evaporating droplet. *Journal of Applied Physics*, 91(10):6406–6415, May 2002.

[6] S. V. Patankar. *Numerical heat transfer and fluid flow.* Hemisphere Publishing, Washington, DC, 1980.